Journal of Energetic Materials
Publication details, including instructions for authors and subscription information:
http://www.informaworld.com/smpp/title~content=t713770432

Calculations and measurements on the flow in unconfined detonation

Graeme A. Leiper[a]; Ian D. Kerr[b]; Michael Kennedy[b]
[a] Nobels Explosives Co. Ltd., Stevenston [b] Health and Safety Executive, Buxton

To cite this Article Leiper, Graeme A. , Kerr, Ian D. and Kennedy, Michael(1989) 'Calculations and measurements on the flow in unconfined detonation', Journal of Energetic Materials, 7: 4, 355 — 380
To link to this Article: DOI: 10.1080/07370658908014904
URL: http://dx.doi.org/10.1080/07370658908014904

CALCULATIONS AND MEASUREMENTS ON THE FLOW IN UNCONFINED DETONATION

Graeme A. Leiper
Nobels Explosives Co. Ltd.
Stevenston

and

Ian D. Kerr and Michael Kennedy
Health and Safety Executive
Buxton

In this work a comparison is made between measured and calculated flows in axisymmetric detonations based on the axial density profile in the detonation, the shockfront radius of curvature of the detonation, and the reaction zone length. Measurements were made using flash radiography, optical photography, and electromagnetic particle velocity gauging in a commercial air-sensitised emulsion explosive at two voidages, each at two charge diameters. Calculations were performed using the alternative approaches of slightly divergent flow theory and a finite element Lagrangian hydrocode. Chemical reaction rate models in the calculations were parameterised against the measured unconfined detonation velocity charge diameter effect. The result of the study was that both modelling techniques gave good agreement with available experimental data, though the slightly divergent flow model was more accurate in the region close to the shock. It has

also been demonstrated that providing the two approaches had been carefully calibrated, the agreement between them was not sensitive to the form of the models used.

INTRODUCTION

Many methods have been proposed for measuring and predicting the performance of condensed explosives, detonating in right cylindrical charges. Each mathematical model yields differing answers for a particular problem and each experimental technique measures a different physical property of the system, yet comparisons between various experimental and theoretical approaches are not common. Such comparisons are essential if a worker is to employ the optimum modelling and measurement techniques for a particular problem. In this work two calculational methods are compared with three measurements made on an air sensitised emulsion explosive at low and high voidages, each at the critical and twice the critical diameter.

Calculations were performed using a slightly divergent flow technique CPEX[1], and a two dimensional finite element hydrocode, DYNA2D[2]. Both employed the same chemical reaction rate model to describe the reactivity of the explosive and the same equation of state for the reaction products. The unreacted equation of state differed slightly due to the solution algorithm used in the two methods, but in either case it well represented the porous hugoniot of the explosive.

Experimental measurements were made on axial density profiles

as measured by flash radiography, on shock front radius of curvature as measured by radiography and optical photography, and on reaction zone lengths and particle velocity profiles as measured by the electromagnetic particle velocity technique.

MODELLING TECHNIQUES

Slightly Divergent Flow

The slightly divergent flow method was first described by Wood and Kirkwood[3]. Fickett and Davis[4] showed it to be a member of a general set of eigenvalue solutions to the standard Zeldovitch - Von Neumann - Doering theory of detonation. In slightly divergent flow, radial motion of the detonation products due to incomplete lateral confinement provides a mechanism for the dissipation of energy, and enables eigenvalue solutions to be reached. This method has been embodied in a detonation model, CPEX[1], which has been fully described elsewhere.

CPEX is formulated as a streamtube model in a shock fixed frame of reference. It is strictly applicable only along the centre line of the charge, i.e. it cannot be used to examine the radial dependence of the flow, but it does not suffer from shock smearing associated with hydrocode techniques. It requires knowledge of the shock radius of curvature to operate, which is given in the form of a generalised relationship between shock radius of curvature, reaction zone length and charge diameter[5].

LAGRANGIAN HYDROCODE

The solution of problems involving shockwaves in inert and

chemically reactive media using Lagragian hydrocode techniques, has been well documented[6]. In this study the hydrocode DYNA2D[2], modified[7] to use chemical reaction rate and product equation of state routines identical to those in CPEX, was used to perform resolved reaction zone simulations of unconfined detonations. The CPEX unreacted equation of state had to be altered for use in DYNA2D to accommodate the hydrocode solution algorithm, and was replaced by a Gruneisen equation of state[7].

The hydrocode method calculated the total flow field in the explosive, but suffered from artificial smearing of the shock front in the solution algorithm. This affected the flow profiles close to the shock. The dimension of the calculational grid altered with the charge diameter being simulated: a minimum of ten cells were used across the charge radius, and the reaction zone in the explosive was resolved to better than 0.25 mm.

Modus Operandi

The analysis procedure employed for both methods was identical. The ideal detonation performance of the explosive, detonation velocity, Chapman-Jouguet state, and isentrope from the Chapman-Jouguet state were calculated from the explosive formulation and initial density, using a JCZ[8] based equation of state and non-stiochiometric chemical equilibrium routine[6]. The isentrope was fitted to a polytropic equation of state in which the polytropic index was a polynomial function of density[1].

The behaviour of the unreacted explosive was modelled using a

porous hugoniot derived from Lattice BKW theory[9], and the mixture rules of Vostoboinikov[10]. This had previously been shown to agree with experimental measurements[5]. In the case of the CPEX model, a polytropic equation of state was used to describe off-hugoniot states in the unreacted explosive, in the case of the hydrocode a Gruneisen equation of state was used.

The reaction rate law in both codes was fitted to the experimental detonation velocity charge diameter effect, by adjusting three fitting constants corresponding to a critical pressure and two reaction time constants, one for the hotspot phase and one for the bulk. In all cases the critical diameter and critical detonation velocity was reproduced to within 5% accuracy (Figure 1). Change necessary to implement the equation of state routines in the two codes resulted in differing rate law parameters being used in each code. This was not thought to affect the results of the study.

EXPERIMENTAL

In all experiments an air sensitised water-in-oil emulsion explosive of composition 78.7% Ammonium Nitrate, 16% Water, and 5.3% Oils and Surfactants was used. The two voidage levels used 17% and 25%, corresponding to densities of 1.06g/cc and 1.14g/cc, were obtained by the addition of hollow glass spheres of diameter between 75μm and 90μm, to the prepared, de-aerated, emulsion. The explosive was cartridged in manilla paper shells in two charge diameters, the critical diameter, and twice the critical diameter

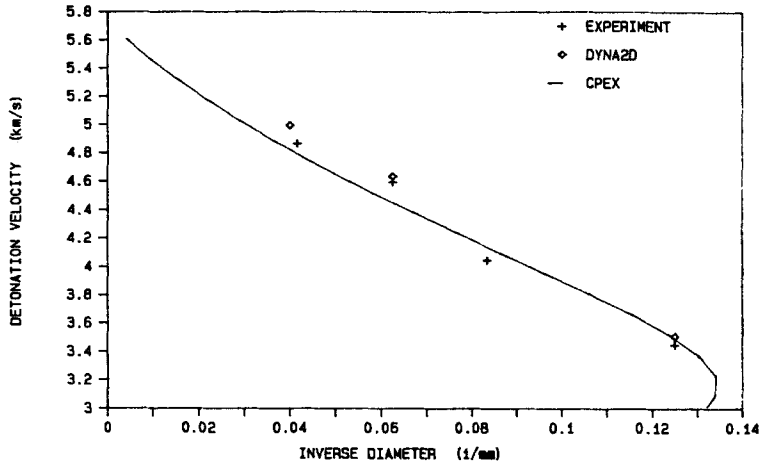

FIGURE 1
Variation of Detonation Velocity with Charge Diameter

i.e. 8mm, 16mm, and 10mm, 20mm, for the high and low voidage compositions respectively. The cartridges were initiated by a commercial 8* detonator and a small Pentolite pellet. The detonation was allowed to run at least 6 charge diameters before any measurements were made.

Flash Radiography

Detonating cartridges were photographed using a 300kV X-ray flash system. The apparatus, which was of the Field Emission type 730/2710 now supplied by Hewlett Packard, produced a flash of approximately 50ns duration when pulsed at a potential of 300kV. The images were recorded using 3M XUD film and TRIMAX 16 intensifying screens, enclosed in a cassette designed so as to protect film and screens from the detonation of the explosive which was between 200mm and 300mm away. The exposed films were developed using Ilford PHENSOL developer in a semi-automatic process.

The experimental design is shown in Figure 2. The twisted wire probe wound round the pentolite pellet acted as a trigger for the X-ray apparatus; the probe was always placed close to the end of the pellet in contact with the emulsion explosive. Immediately before detonation was initiated in the Pentolite, a potential difference of 110 volts was applied to the wires of the probe so that as soon as the detonation wave caused the necessary conditions at the probe, an electrical pulse would be produced, which, with the aid of a delay unit, was used to initiate the flash X-ray at various times later. In all experiments, the cartridge was placed

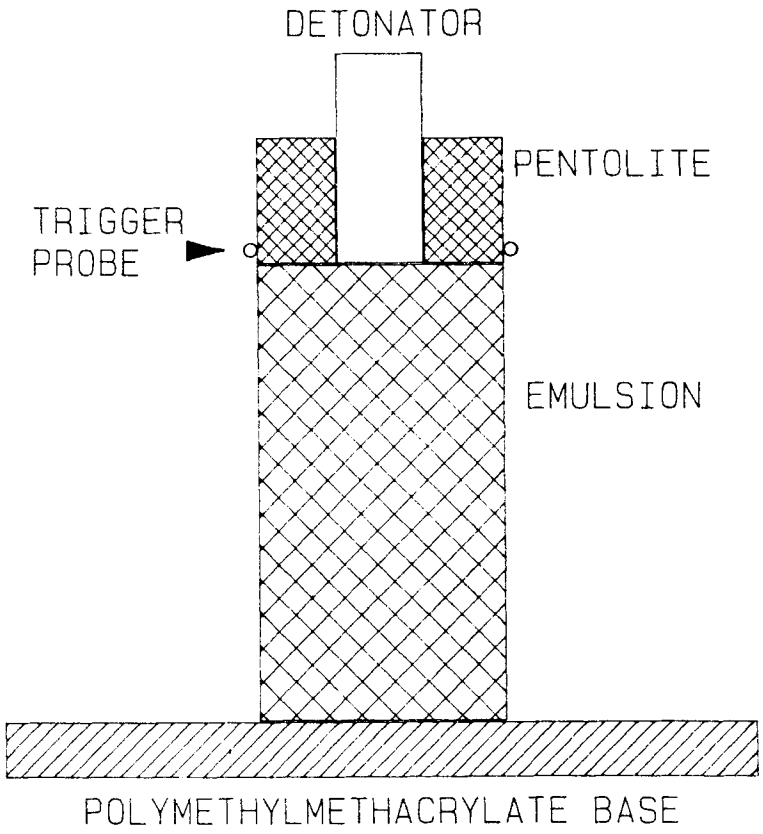

FIGURE 2
Experimental Arrangement for Flash Radiography
Not to scale

2.35m from the X-ray tube.

Image data were acquired from the sciagrams by means of an Optronics P-1000 rotating drum scanner which was used to scan the region of interest of each sciagram, and record the measured optical density values as a 256 by 256 array of numbers for processing using a microcomputer system which was coupled to a framestore. A typical image of a 20mm diameter cartridge acquired and stored in this way is shown in Figure 3. The curved detonation wave in the centre can be seen moving into the undetonated explosive in the lower half of the image.

The following methods which were used for computer image analysis have been described more fully previously[11,12]. The sciagram image was calibrated in terms of optical densities versus integrated explosive densities over the measured pathlengths by using data gathered from the image of the undetonated explosive immediately ahead of the position of the wavefront. A satisfactory estimate of the coordinates of the wavefront was obtained by, in effect, subtracting an image of the undetonated explosive from that of the detonated explosive. The difference image that resulted, and from which noise fluctuations had been removed by a thresholding operation, was processed in the computer to produce coordinates of the wave front position. Assuming axial symmetry for the wave, these coordinates were then used in conjunction with the calibration data from the original image to produce estimates of the average material densities at all positions behind the

FIGURE 3
Typical Flash Radiiograph

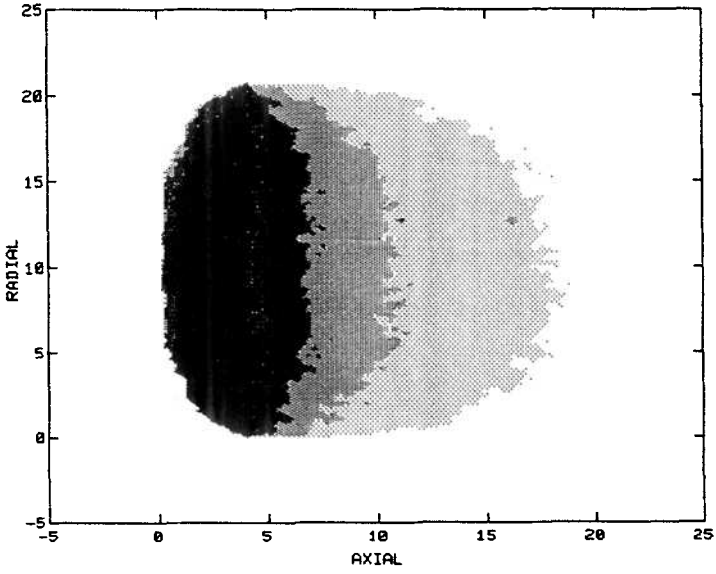

FIGURE 4
Contour Plot of Processed Radiograph

wavefront. A typical density contour resulting from the analysis is displayed in Figure 4. Note that the contour plot reflected both a distribution of intial density through the charge and natural fluctuations in the detonation process in the explosive.

Detonation Velocity Measurements

Detonation velocity measurements were made using the time of flight of the shockwave in the explosive between two fibre optic probes 200mm apart. Each probe consisted of a length of 1mm diameter plastic optical fibre, one end of which was inserted into a thin walled aluminium end cap that acted as an air gap which luminesced upon arrival of the shock. The other end was terminated by a fast responding photo-diode to provide an electrical switch to gate a digital timer.

The critical diameter was ascertained by finding the minimum diameter in which detonation would propagate. This was performed separately from the detonation velocity measurement, to prevent the probes disturbing the flow.

Optical Photography

Optical streak photography was used to measure the shape of the shockfront as it emerged from the end of the explosive cartridge. An Imacon 790 image converting camera was used to perform the measurements. Streak records were digitised manually on a microcomputer bitpad and the central 20° arc of the profile was fitted to a circle. These measurements have been reported previously[5].

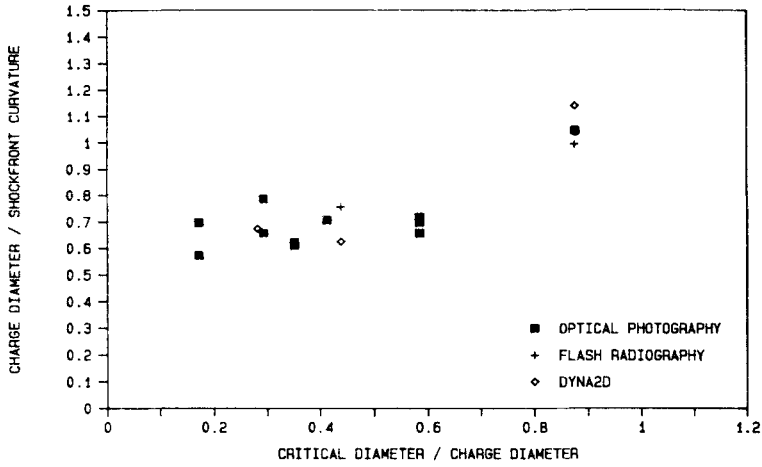

FIGURE 5
Shockfront Curvature in Low Density emulsion

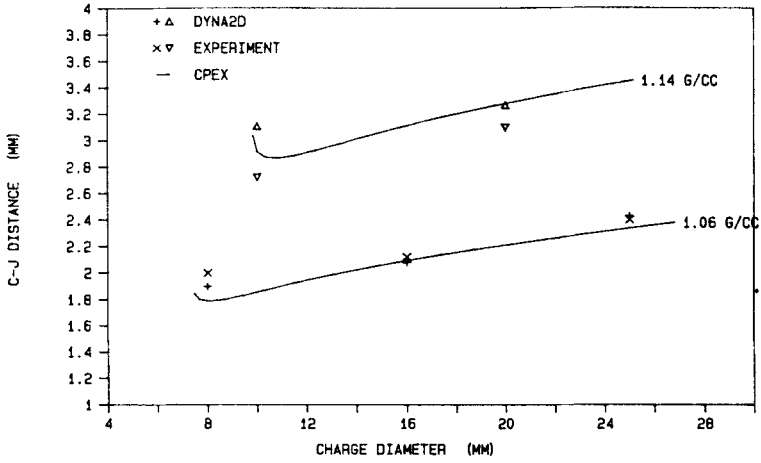

FIGURE 6
Reaction Zone Length as a Function of Charge Diameter

Particle Velocity Measurements

The electromagnetic particle velocity technique had previously been used to measure the reaction profiles in the compositions and charge diameters of interest[5]. The gauge traces were reanalysed to determine the particle velocity profile in the detonation, and the pathological (sonic) point in the flow.

DISCUSSION

It was the object of this work to asses the ability of very different calculational schemes to predict the flow in steady state detonations, given that the data used to parameterise the reaction rate models in the schemes was identical. The comparison was based on three criteria, the ability of the models to calculate the flow in the shocked unreacted explosive, the ability of the models to couple the chemical exothermicity to the flow, and the ability of the models to represent the behaviour of the detonation products after reaction had occurred. These benchmarks were reflected in one or more of the measurements made on the explosive. Variation of the initial density of the explosive provided sufficiently different reaction and flow behaviours that the comparison could be regarded as of a general nature.

The first comparison that was made was on the variation of shockfront radius of curvature with charge diameter. The shock front curvature as measured optically and by flash radiography, was plotted along with that predicted by DYNA2D (Figure 5). The data from the hydrocode was analysed in the same manner as the streak

photographs. The generally good agreement extended over the diameter and voidage range used, though the scatter in the experimental data made quantitative assessments impossible.

It can be inferred from these results that the unreacted equation of state and mixture rules in the hydrocode were adequately representing the local sound speed in the area close to the shockfront. However edge effects which were clearly visible in the optical and radiographic records were much reduced in the hydrocode data; this was attributed to deficiencies in the unreacted equation of state in areas of strong rarefaction,i.e. where unreacted material had moved far from its hugioniot state.

The next point of reference to be used was the calculation of the pathological or sonic plane in the flow i.e. the position behind the shock where sonic communication with the shock was lost. This two-dimensional analogue of the Chapman-Jouguet point was quantified into a single value by ascertaining the position of the pathological point on the charge axis, and calling this the 'CJ distance'. The variation of 'CJ distance' with charge diameter was calculated and compared to values measured using the electromagnetic gauge technique. Both CPEX and DYNA2D reproduced the correct form for the dependance of 'CJ distance' on charge diameter. They were in good agreement with each other, and were within experimental error of the measured values (Figure 6). As the pathological point is controlled by the mixture equation of state of the reacting explosive,by the chemical reaction rate, and

by the coupling of energy between the chemical exothermicity and the hydrodynamic flow, the agreement provided strong validation of the two calculational proceedures.

A comparison was also made between the measured particle velocity profiles and those predicted by CPEX and DYNA2D (Figure 7). The CPEX predictions were found to be in good agreement with the gauge traces. In the DYNA2D simulations it was clear that artificial viscosity and the algorithm used for negating its effect on the chemical reaction rate, first caused an overshoot in the predicted profile followed by a compensating abrupt fall. This was also reflected in the density calculations discussed below.

Density profiles measured by flash radiography provided data to check the overall combination of reaction rate,equation of state and mixture rule models. For the densities and charge diameters of interest, the sciagrams resolved the flow field from the shockfront through to the point at which the chemical reaction had either proceeded to completion or had been frozen by expansion processes ocurring in the flow. The radiographic data however required careful interpretation. For clarity the comparison between calculation and measurement has been made in two stages.

At all density and diameter combinations the radiographic data has been displayed with the CPEX prediction (Figures 8,9). In three cases 8mm, 10mm, and 20 mm the calculated density was higher than measured close to the shockfront, in good agreement over a short range, and then again higher than the measurements far from

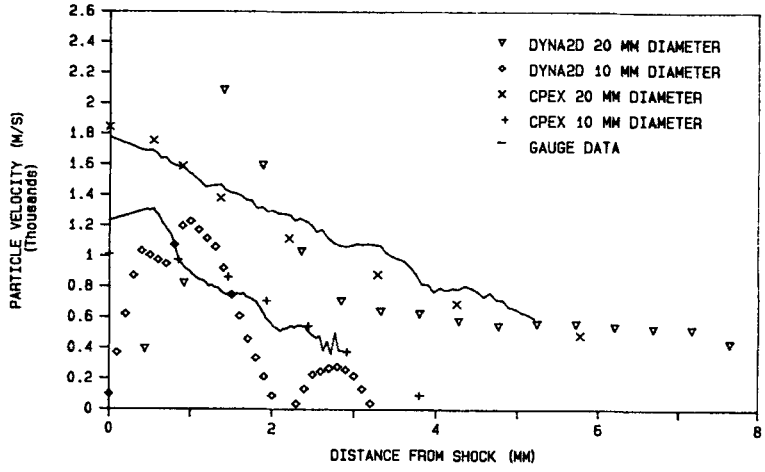

FIGURE 7
Particle Velocity Profiles in High Density Emulsion

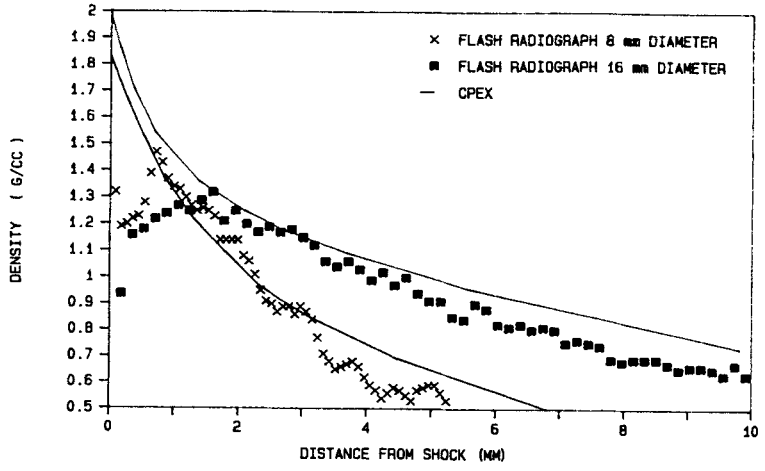

FIGURE 8
Density Profile for Low Density Emulsion
CPEX vs Radiographic Data

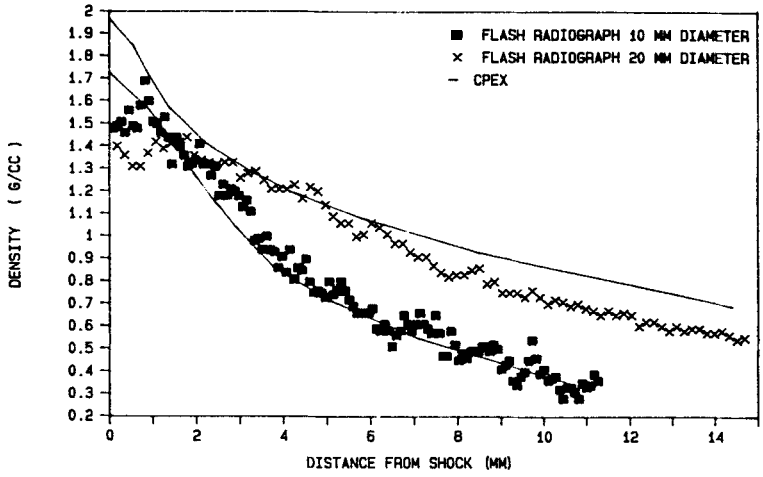

FIGURE 9
Density Profile for High Density Emulsion
CPEX vs. Radiographic Data

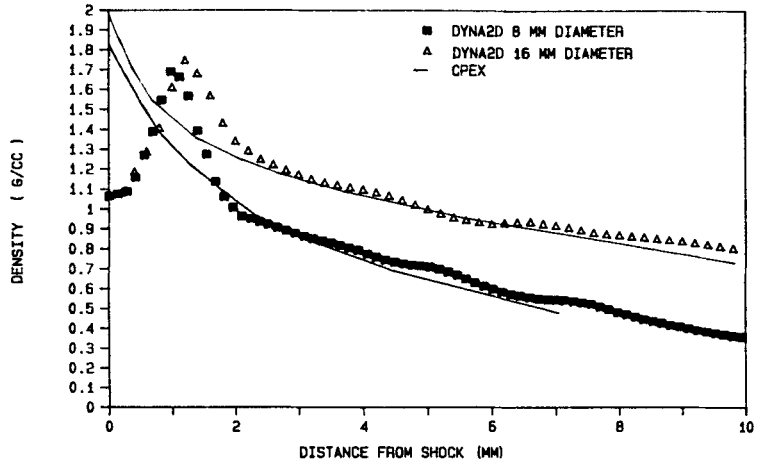

FIGURE 10
Density Profile for Low Density Emulsion
CPEX vs DYNA2D

the shock. In the case of the 10mm. diameter cartridge, the CPEX prediction was higher than measured close to the shock but then in good agreement at all other distances. A similar trend was noted with the DYNA2D predictions. Apart from the area in which the artificial viscosity was active there was good agreement between CPEX and DYNA2D (Figure 10).

The apparent lack of agreement between CPEX or DYNA2D and the radiographic data was partly caused by smearing due to motion of the shock during exposure of the X-ray film, partly due to the finite beam width of the X-ray generator, and partly due to spatial averaging inherent in radiography. The exposure time of 50ns resulted in the detonation wave travelling 0.2mm during radiography. The X-ray beam was conical in nature and emanated not from a point but from a finite aperture, causing a beam smear of 0.5mm at the cartridge position. The smearing due to these effects was axial in nature and therefore would have been most significant in regions of large axial density gradients, i.e. close to the wave front.

Spatial averaging in the radiographs was significant in all regions where there was a strong radial dependency in the flow field. The flow codes calculated the true axial density profile:

$$\sigma(z) = \sigma(z), \quad r=0 \qquad 1$$

but the radiographs yielded :

$$\sigma(z) = \frac{1}{R}\int_0^R \sigma(z,r)dr \qquad 2$$

Thus if there was a large radial variation in density, the

radiography acted to spatially average the data. This radial averaging increased the discrepancy at the shock front, and caused all of the apparent error in the calculated profiles far from the shock.

The flow field in a typical detonation, was calculated by DYNA2D (Figure 11). Close to the shock there was a significant radial density gradient. This gradient flattened out on moving back from the shock , as the isopicnics changed from convex to concave. Far from the shock, lateral expansion was well developed and there again exsisted a strong radial density dependence. The areas of greatest error between flow calculations and measurements thus corresponded to those areas in which there were strong radial flow gradients. The anomolous agreement found in the case of the 10mm cartridge, was due to the detonation being very close to the critical point. Under this condition the reaction zone was greatly extended, viz the DYNA2D simulation (Figure 12). The effect of this extension of the reaction zone was two fold. The shock appeared effectively thicker to the x-ray beam, so the measured density and calculated densities agreed, even close to the shock front, and the inflection point in the isopicnic radius of curvature occurred farther back in the flow, creating a large area in which there was little radial dependence in the flow. Further, the chemical reaction was so slow that inward moving lateral rarefactions froze the reaction so as to leave a high density low pressure shell of unreacted explosive around the expanding detonation products. This

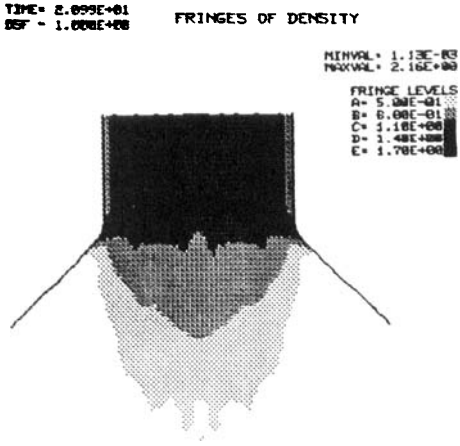

FIGURE 11
DYNA2D Density Fields at 20mm

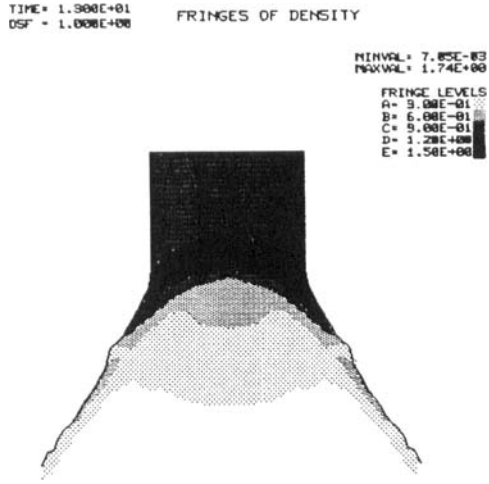

FIGURE 12
DYNA2D Density Fields at 10mm

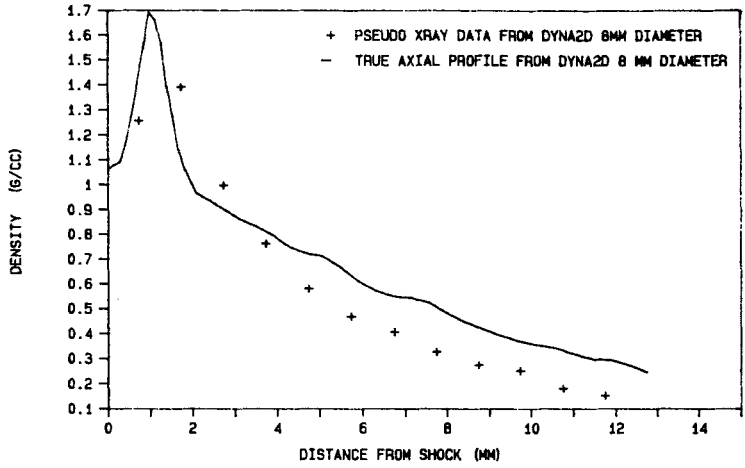

FIGURE 13
DYNA2D Axial Density Profiles vs Pseudo X-Ray Data for
8mm Diameter Charge

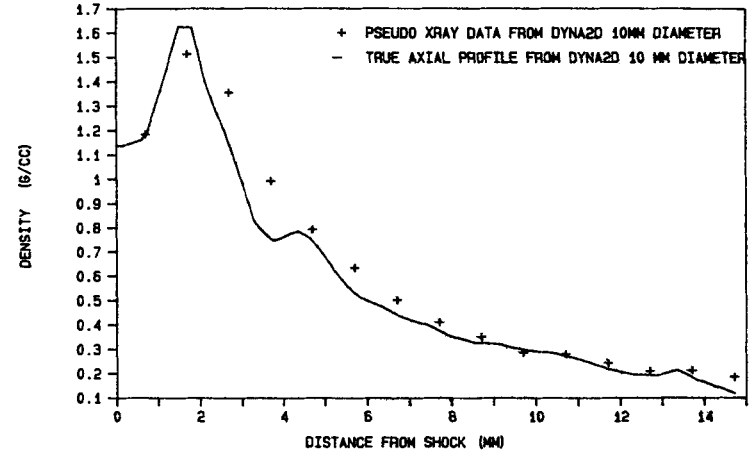

FIGURE 14
DYNA2D Axial Density Profiles vs Pseudo X-Ray Data for
10mm Diameter Charge

shell acted to weight the spatial density average toward the value at the charge axis.

This reasoning was tested by constructing a pseudo x-ray picture from the hydrocode density fields using equation (2), and comparing the pseudo x-ray data with the axial data (Figures 13,14). Features present in the real data were present in the reconstruction: the 8mm data displayed the three areas of error,agreement and error on moving back from the shock, but the 10mm data showed good agreement at all distances. This confirmed the hypothesis, and by implication, vindicated the DYNA2D and CPEX calculations.

Moreover, the ability of the rate law to predict accurately the freezing of reaction due to lateral expansion had been demonstrated.

SENSITIVITY TO CONSTITUTIVE AND RATE MODELS

Up to this point the hydrocode and divergent flow codes had been constrained to use the same constitutive and chemical reaction rate laws. The effects of removing such constraints were now examined.

CPEX and DYNA2D were used to model the performance of the condensed intramolecular explosive Pentolite. As before both codes were required first to reproduce the measured detonation velocity charge diameter dependence of the composition. CPEX was used exactly as before, but DYNA2D was run using the JWL equation of state for the unreacted and reacted explosive[13], and a type of

Ignition and Growth reaction rate model[7]. Again the comparison was on the predicted axial density profile at close and far from the critical diameter (Figure 15).

Somewhat surprisingly, apart from the region close to the shock where the artificial viscosity in DYNA2D was active, there was excellent agreement between the two calculations. Some effects of the reaction rate model were noticeable in the 3mm diameter simulation: at 2mm from the shock there was a plateau in the DYNA2D density profile, associated with the reaction proceeding from being PETN dominated to TNT dominated. The excellent correlation between the two simulations demonstrated that if the rate law parameterisation is adequately performed, different models need not give differing answers.

CONCLUSIONS

The ability of the two different calculational approaches to describe steady-state axisymmetric detonation has been demonstrated against a variety of experimental measurements. The use of detonation velocity-charge diameter data for calibration of the reaction rate models in the codes was found adequate for predicting the steady-state flow in the explosive. Good agreement was found between the two methods, and experiment, for all available data. The detail in the simulations was such that anomalies in the experimental data could be rationalised in terms of the reaction process ocurring in the explosive.

The two methods were used to examine the effect on the predicted

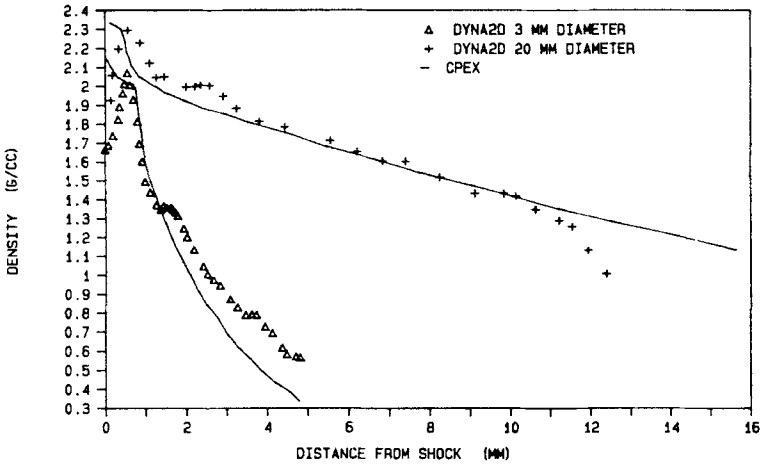

FIGURE 15
Axial Density Profiles for DYNA2D and CPEX in Pentolite
3mm and 20mm Diameter Charges

flow of changes in the reaction rate and equation of state models. Providing adequate parameterisation of the models against experimental data was performed, the agreement between the two approaches was not sensitive to the form of the model used.

ACKNOWLEDGEMENTS

The authors wish to thank Miss A. Steele for preparing the explosive charges and Dr. D.L. Kennedy for providing the hydrocode results on Pentolite. The permission of I.C.I PLC. and the Health and Safety Executive to publish this paper is gratefully acknowledged.

REFERENCES

1. I.J. Kirby and G.A. Leiper in "Proceedings of the Eighth Symposium (International) on Detonation", Office of Naval Research, Washington, 1985
2. J.O. Hallquist, " A Users manual for DYNA2D - An Explicit Two-dimensional hydrodynamic Finite Element Code with Interactive Rezoning", Lawrence Livermore Laboratory, Livermore, 1982
3. W.W. Wood and J.G. Kirkwood, J. Chem. Phys., 22, p1920
4. W. Fickett and W.C. Davis, "Detonation", Univ. of Calif., Berkley, 1978
5. G.A. Leiper et al, in "Proceedings of the Eighth Symposium (International) on Detonation", Office of Naval Research, Washington, 1985
6. C.L. Mader, "Numerical Modelling of Detonation", Univ. of

Calif., Berkley, 1977

7. D.L.Kennedy, private communication
8. M. Cowperthwaite and W.H. Zwisler, in "Proceedings of the Sixth Symposium (International) on Detonation", Office of Naval Research, Washington, 1985
9. C.M. Lownds, private communictaion
10. Vostoboinikov, et al, Combustion Explosion and Shock Waves, 3(4), p359
11. M. Kennedy and I.D. Kerr in "Proceedings of 16th. International Congress on High Speed Photograhy and Photonics", S.P.I.E. 491,1981
12. M. Kennedy and I.D. Kerr in "Proceedings of 17th. International Conference of ICT",1986"
13. J. Kury, et al, in "Proceedings of the Fourth Symposium (International) on Detonation", Office of Naval Research, Washington, 1965